Filaggrin Deficiency Leads to Impaired Lipid Profile and Altered Acidification Pathways in a 3D Skin Construct

Kateřina Vávrová[1], Dominika Henkes[2], Kay Strüver[3], Michaela Sochorová[1], Barbora Školová[1], Madeleine Y. Witting[3], Wolfgang Friess[3], Stephan Schreml[4], Robert J. Meier[5], Monika Schäfer-Korting[2], Joachim W. Fluhr[6] and Sarah Küchler[2]

Mutations in the filaggrin (*FLG*) gene are strongly associated with common dermatological disorders such as atopic dermatitis. However, the exact underlying pathomechanism is still ambiguous. Here, we investigated the impact of FLG on skin lipid composition, organization, and skin acidification using a *FLG* knockdown (*FLG* −) skin construct. Initially, sodium/hydrogen antiporter (NHE-1) activity was sufficient to maintain the acidic pH (5.5) of the reconstructed skin. At day 7, the FLG degradation products urocanic (UCA) and pyrrolidone-5-carboxylic acid (PCA) were significantly decreased in *FLG* − constructs, but the skin surface pH was still physiological owing to an upregulation of NHE-1. At day 14, secretory phospholipase A$_2$ (sPLA$_2$) IIA, which converts phospholipids to fatty acids, was significantly more activated in *FLG* − than in *FLG* + . Although NHE-1 and sPLA$_2$ were able to compensate the FLG deficiency, maintain the skin surface pH, and ensured ceramide processing (no differences detected), an accumulation of free fatty acids (2-fold increase) led to less ordered intercellular lipid lamellae and higher permeability of the *FLG* − constructs. The interplay of the UCA/PCA and the sPLA$_2$/NHE-1 acidification pathways of the skin and the impact of FLG insufficiency on skin lipid composition and organization in reconstructed skin are described.

INTRODUCTION

Filaggrin (*FLG*) loss-of-function mutations contribute to several dermatological disorders such as ichthyosis vulgaris and atopic dermatitis (AD) (Palmer *et al.*, 2006; Brown and McLean, 2012). Mutations in the *FLG* gene are the most widely occurring genetic risk factors for AD known to date and have been identified in up to 20–40% of the patients

[1]Faculty of Pharmacy, Charles University in Prague, Hradec Kralove, Czech Republic; [2]Institute for Pharmacy, Pharmacology and Toxicology, Freie Universität Berlin, Berlin, Germany; [3]Department of Pharmacy, Ludwig-Maximilians University Munich, Munich, Germany; [4]Department of Dermatology, University Medical Center Regensburg, Regensburg, Germany; [5]Institute of Analytical Chemistry, Chemo- and Biosensors, University of Regensburg, Regensburg, Germany and [6]Department of Dermatology, Charité University Clinic, Berlin, Germany

Correspondence: Sarah Küchler, Institute for Pharmacy, Pharmacology and Toxicology, Freie Universität Berlin, Königin-Luise-Strasse 2–4, Berlin 14195, Germany. E-mail: sarah.kuechler@fu-berlin.de

Abbreviations: AD, atopic dermatitis; Cer, ceramides; FLG, filaggrin; GCer, glucosylceramide; GCerase, β-glucocerebrosidase; GSph, glucosylsphingosine; NHE-1, sodium/hydrogen antiporter; P$_{app}$, mean apparent permeability coefficient; PCA, pyrrolidone-5-carboxylic acid; PL, phospholipid; SC, stratum corneum; SM, sphingomyelin; SMase, sphingomyelinase; SPC, sphingosylphosphorylcholine; sPLA$_2$, secretory phospholipase; UCA, urocanic acid

(Palmer *et al.*, 2006; Jung and Stingl, 2008; O'Regan *et al.*, 2009). Although *FLG* mutations are the most common mutations in these skin disorders, still the overall impact on the pathogenesis is not fully understood.

FLG is crucial for the adequate development of the epidermal structure and barrier function (Brown and McLean, 2012). It is ultimately degraded to its component amino acids including histidine. These amino acids are highly hygroscopic and are the major components of the ''natural moisturizing factor,'' which is crucial for epidermal hydration and barrier function (Rawlings and Harding, 2004). Histidine is of particular importance as it is eventually metabolized to urocanic acid (UCA) and pyrrolidone-5-carboxylic acid (PCA), which contribute to the acidification of the stratum corneum (SC) via the ''histidine-to-UCA/PCA pathway'' (Krien and Kermici, 2000; Fluhr and Elias, 2002). Furthermore, because of the importance of the acidic pH for the formation of the acidic mantle, other pathways contribute to its formation (Fluhr *et al.*, 2010). This includes the sodium/hydrogen antiporter-1 (NHE-1) and the phospholipid (PL)-to-free fatty acids (FFA) pathways via secreted phospholipases (sPLA$_2$) (Fluhr and Elias, 2002; Chan and Mauro, 2011). However, until now the interplay and impact of the single pathways on the formation of the acidic skin surface pH remain unclear. The acidic mantle is a prerequisite for the formation of ceramides (Cer), i.e., the most important lipid class in the SC

intercellular lipid matrix, and, thus, directly influences the skin barrier development: In the SC the β-glucocerebrosidase (GCerase) and acid sphingomyelinase (SMase) metabolize glycosylceramides (GCer) and sphingomyelin (SM) to Cer. Both enzymes require an acidic environment of $pH \leqslant 5.5$ for their optimal activity (Feingold, 2007). Thus, a decreased production of UCA/PCA due to a lack of FLG could result in an increase of SC pH and, consequently, to a decreased Cer content. This assumption was underlined by the reduced Cer levels found in AD patients (Imokawa *et al.*, 1991; Di Nardo *et al.*, 1998; Bleck *et al.*, 1999; Ishikawa *et al.*, 2010; Park *et al.*, 2012).

We have previously described a *FLG* knockdown (*FLG* –) skin construct, which exhibits disturbed epidermal maturation and differentiation, increased susceptibility to irritants, and altered drug absorption (Küchler *et al.*, 2011). In this study, we investigated how the lack of FLG influences the composition and organization of the SC lipids generated in *FLG* – constructs in comparison to normal skin constructs and isolated human SC and how skin absorption is influenced. In addition, we determined the amount of UCA/PCA, the expression of various $sPLA_2$ subtypes, and of the sodium-hydrogen antiporter NHE-1, $sPLA_2$ activity, and the skin surface pH in a time-dependent manner to gain deeper insights in the mechanisms of skin acidification.

RESULTS

FLG – constructs contain significantly less UCA and PCA compared to healthy skin models

The knockdown efficiency of our *FLG* – constructs was $75.7 \pm 2.83\%$ ($n = 10$; Supplementary Figure S5 online). As expected, *FLG* knockdown decreased the levels of the histidine degradation products PCA (*FLG* + 0.45 ± 0.05 mmol g^{-1} protein; *FLG* – 0.22 ± 0.04 mmol g^{-1} protein) and UCA (*FLG* + 0.018 ± 0.003 mmol g^{-1} protein; *FLG* – 0.011 ± 0.002 mmol g^{-1} protein) at day 14 (Supplementary Figure S1 online). Similar differences were detected at day 7, but not at day 4 (Supplementary Figure S4). In comparison to human skin (UCA 0.210 ± 0.045 mmol g^{-1} protein; PCA 2.65 ± 0.42 mmol g^{-1} protein), PCA and UCA levels were reduced.

FLG – constructs show significant upregulation of NHE-1 and $sPLA_2$ IIA

We found a significant upregulation of NHE-1 in the *FLG* – constructs compared to *FLG* + starting at day 7. No significant differences were seen at day 4 on the mRNA (Figure 1a) and protein level (data not shown). $sPLA_2$ IIA was only found at day 14 in the constructs; its relative expression being significantly higher in the *FLG* – construct (Figure 1a). The upregulation of $sPLA_2$ IIA and NHE-1 was further confirmed on the protein level (Figure 1b and Supplementary Figure S3 online). $sPLA_2$ IB, IIF, V, and XIIA were detected, too, some of them are only expressed at day 14 and without statistically significant differences between *FLG* + and *FLG* – , respectively (Supplementary Figure S2 and Supplementary Table S1 online). Because of the relatively small difference in $sPLA_2$ IIA on mRNA level, we also checked for the activity of the enzyme detecting about 55% increased $sPLA_2$
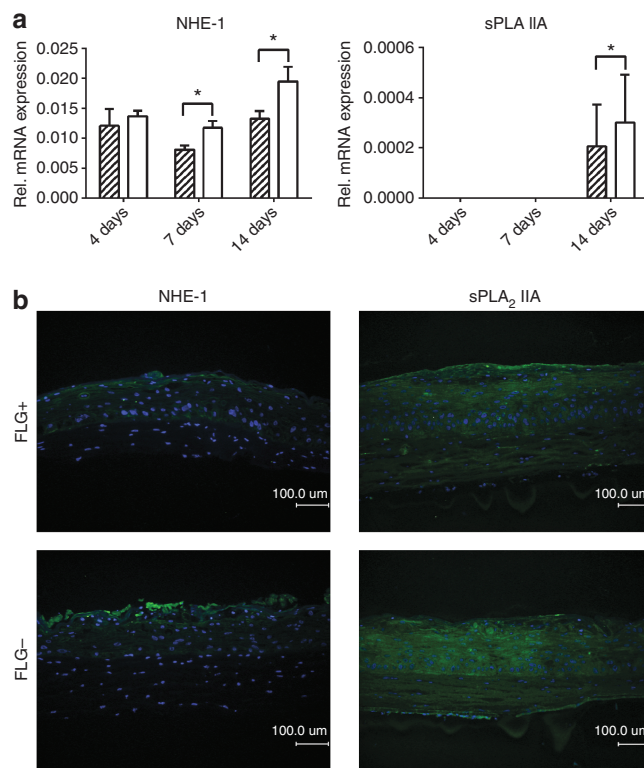
Figure 1. **Sodium/hydrogen antiporter (NHE-1) and secretory phospholipase A₂ ($sPLA_2$) IIA expression.** (**a**) Sodium/hydrogen antiporter (NHE-1) and secretory phospholipase A₂ ($sPLA_2$) IIA expression. Relative mRNA expression of NHE-1 and $sPLA_2$ IIA in *FLG* + (striped bars) and *FLG* – (white bars) constructs at days 4, 7, and 14, quantified using reverse transcription PCR (RT-PCR). Mean ± SEM, $n = 10$, *$P \leqslant 0.05$. (**b**) In *FLG* – constructs, the expression of NHE-1 and $sPLA_2$ IIA at day 14 is clearly increased (green fluorescence). The nuclei were stained with 4′,6-diamidino-2-phenylindole (DAPI) (blue fluorescence) (bar = 100 μm). FLG, filaggrin.

activity in *FLG* – (36.28 ± 10.70 U ml^{-1}) compared to *FLG* + (23.38 ± 7.70 U ml^{-1}).

No differences of skin surface pH were found in *FLG* + and *FLG* –

Interestingly, we measured a physiological skin surface pH around pH 5.5 from day 4 through day 14 of tissue cultivation. No differences were detected between the *FLG* + and *FLG* – constructs. The respective absolute values are given in Figure 2 and measurement controls are depicted in Supplementary Figure S6 online.

FLG knockdown leads to a less ordered skin lipid barrier

The lipid chain order in the SC sheets from normal and *FLG* – constructs was examined by attentuated total reflectance-Fourier transform infrared spectroscopy and compared to hydrated human SC. Cultivated for 7 days, the constructs displayed more disordered lipid chains than the human SC, as indicated by the shift of both the methylene symmetric and asymmetric stretching vibrations towards slightly higher wavenumbers (over 2,851 and $\sim$2,921 cm^{-1}, respectively, compared to 2,850 and 2,918 cm^{-1} in human SC) and significant broadening of both bands due to incorporation of more *gauche* conformers into the lipid chains (Mendelsohn and
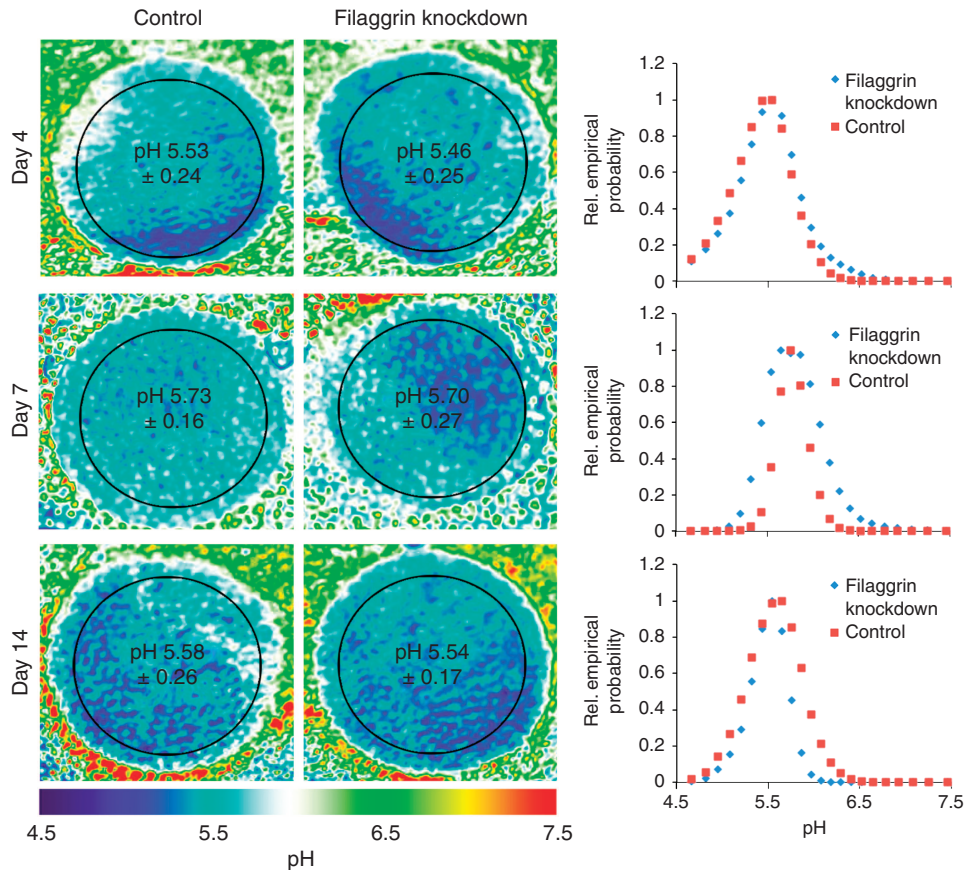
Figure 2. Skin surface pH of *FLG*+ (control) and *FLG*− (FLG knockdown) constructs at day 4, 7, and 14 of tissue cultivation and a histographical analysis of the spatial surface pH value distributions of the skin constructs using RGB imaging luminescent 2D imaging. Regions of interest are marked with circles, and the respective mean pH values ± SD are given. No differences were observed between *FLG*+ and *FLG*− at day 4 ($n=2$), day 7 ($n=4$), and day 14 ($n=4$), respectively. FLG, filaggrin.

Moore, 2000); (Figure 3). No differences were found between *FLG*+ and *FLG*− cultures at day 7.

In contrast, cultivation for 14 days led to significant differences between the lipid chain conformations of the constructs. While the normal cultures showed a trend toward improving the lipid chain order reflected by lower wavenumbers of methylene stretching bands and decreased bandwidths, the opposite was found for *FLG*−. The methylene symmetric stretching in the *FLG*− construct reached ~2,852 cm^{-1}, indicating a higher proportion of a liquid ordered phase (Velkova and Lafleur, 2002) where the lipid chains are still more ordered than in the fluid phase but display greater lateral and rotational freedom. This is consistent with the character of the methylene scissoring mode, which appeared as a single band at around 1,466 cm^{-1}, indicating a laterally disordered phase. The relative amounts of lipids, determined as the corrected area under the C–H stretching vibration, and also the lipid/protein ratios, were similar in both models.

FLG− constructs contain more FFA compared to normal constructs

The total lipid content was very similar in both *FLG*− and *FLG*+ constructs (approximately 100 µg mg^{-1} of dry SC). No differences were found between the 7 day models consistent with the FTIR results and Mildner *et al.*, (2010). After a 14 day cultivation of *FLG*+ constructs, the amounts of the major barrier lipids FFA (11.3 ± 2.1 µg), Chol (12.5 ± 2.1 µg), Cer (21.1 ± 3.7 µg), and cholesterol sulfate (1.3 ± 0.5 µg) per mg of SC (Figure 4a) correspond to a roughly equimolar mixture of FFA, Chol, and Cer, which is in agreement with previous studies (Wertz, 2000). Yet, the amount of these barrier lipids was significantly lower in either construct than in human SC (Figure 4a). In the skin models, significant amounts of more polar lipid precursors including SM, GCer, and PL were detected, explaining the lower lipid chain order of the *in vitro* constructs compared to human SC.

In *FLG*− cultivated for 14 days, all these lipid classes were found, too. The only significant difference between *FLG*− and *FLG*+ was an almost 2-fold increase in FFA (21.9 ± 3.6 µg mg^{-1}) accompanied by slightly less PL (22.3 ± 5.8 µg mg^{-1}) (Figure 4a), suggesting an increased PL processing into FFA by sPLA$_2$. Importantly, neither glucosylsphingosine (GSph) nor sphingosylphosphorylcholine (SPC), i.e., the degradation products of SM and GCer found previously in AD (Hara *et al.*, 2000), was detected.
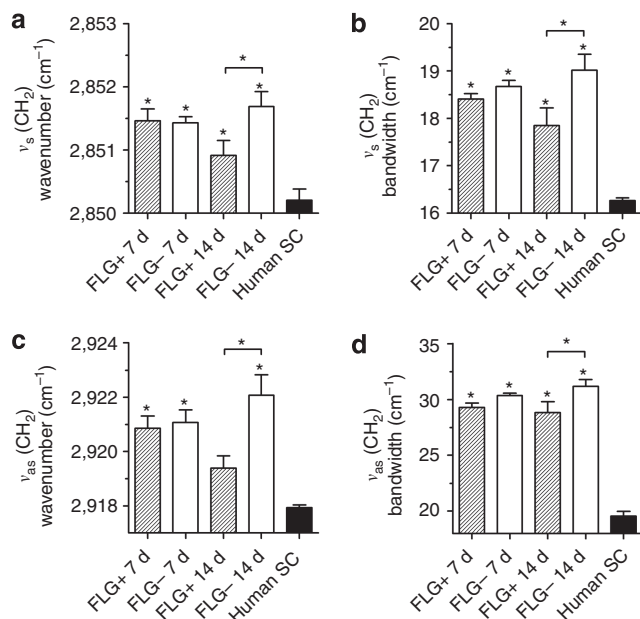
Figure 3. Stratum corneum (SC) lipid chain order as indicated by the wavenumbers of the infrared (IR) methylene symmetric (v_s) and asymmetric (V_{as}) stretching vibrations (a and c) and their corresponding bandwiths (b and d) of the hydrated SC samples from normal (*FLG+*) and *FLG* knockdown (*FLG−*) skin models grown for 7 and 14 days compared to isolated human SC. The hydrated SC samples were examined by attentuated total reflectance-Fourier transform IR (ATR-FTIR) spectroscopy by coaddition of 256 scans at $4 \, cm^{-1}$ resolution at $23 \, °C$. Mean ± SEM, $n = 8$. *Statistically significant differences compared to human SC or as indicated at $P \leqslant 0.05$. FLG, filaggrin.
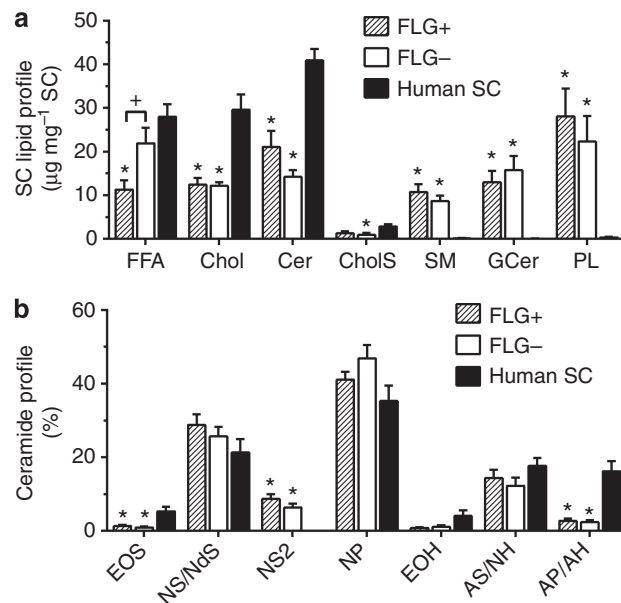

Figure 4. The stratum corneum (SC) (a) lipid content and (b) ceramide (Cer) profiles in *FLG+* and *FLG−* reconstructed skin grown for 14 days compared to human SC. The analyses were performed on silica gel 60 high-performance thin-layer chromatography (HPTLC) plates and quantitated by densitometry after dipping in 7.5% $CuSO_4$, 8% H_3PO_4, and 10% MeOH in water for 10 seconds and heating at $160 \, °C$ for 30 minutes. Free fatty acids (FFA), and cholesterol (Chol) were separated using chloroform/methanol/acetic acid 190:9:1.5 (v/v/v) twice to the top of the plate. The other lipids were separated using chloroform/methanol/acetic acid/water 65:25:6:3 (v/v/v). Mean ± SEM, $n > 17$. *Indicates statistically significant differences compared to human SC at $P \leqslant 0.05$. [+] Statistically significant differences between *FLG+* and *FLG−* skin models at $P \leqslant 0.05$. AS, α-hydroxy sphingosine; CholS, cholesterol sulfate; EOS, ceramide 1; FLG, filaggrin; GCer, glucosylceramide; NP, phytoceramide; NS, non-hydroxy sphingosine; PL, phospholipid.

FLG− constructs display similar Cer profiles compared to *FLG+* control

The overall Cer profiles were similar in both *in vitro* skin models (Figure 4b). The major Cer species in the skin constructs were Cer NS and NP ($28.8 \pm 0.3\%$ and $41.1 \pm 2.1\%$, respectively), which is similar to native human SC, where these Cer species accounted for $21.3 \pm 3.6\%$ and $35.3 \pm 4.2\%$, respectively. The band below Cer NS was assigned to its shorter analog ($8.7 \pm 1.3\%$, labeled as Cer NS2). Such a subfraction of Cer NS was not present in human SC but was detected in reconstructed epidermal models previously (Ponec, 2002; Pappinen *et al.*, 2008). The more polar Cer bands attributed to hydroxylated Cer AS/NH and Cer AP/AH, constituted $14.4 \pm 2.3\%$ and $2.7 \pm 0.6\%$ of the Cer mass compared to $17.7 \pm 2.1\%$ and $16.2 \pm 2.7\%$ in human SC, respectively. The AcylCer species, i.e., EO-type Cer, were found in some but not all lipid models. The mean levels were around 1% for either EOS or EOH, which is lower than in human SC, where they comprised 4 to 5%. Cer EOP concentrations were below the detection limit. The highest amounts of Cer EOS and EOH detected were 4.9 and 3.4% with no significant differences between the skin constructs.

Notably, the percentages of all sphingosine-based Cer (i.e., CerEOS, NS, NS2, and AS) were slightly lower in the *FLG−* constructs but without statistical significance.

Skin permeability is increased in *FLG−* for lipophilic agents

We also determined the permeability of the skin constructs. Testosterone ($\log P = 3.47$) served as lipophilic and caffeine ($\log P = -0.08$) as a hydrophilic model drug. At day 7, neither for testosterone nor caffeine significant differences in skin permeability were found in *FLG+* and *FLG−*. For testosterone, mean apparent permeability coefficients (P_{app}) ± SEM were $5.01 \pm 0.37 \times 10^{-6}$ (*FLG+*) and $5.13 \pm 0.31 \times 10^{-6}$ $cm \, s^{-1}$ (*FLG−*). For caffeine, P_{app} values were $9.33 \pm 0.51 \times 10^{-6}$ for *FLG+* and $10.03 \pm 0.93 \times 10^{-6} \, cm \, s^{-1}$ for *FLG−*. At day 14, significantly higher skin permeability was found for testosterone in *FLG−* in our previous work, whereas no differences were detected for caffeine (Küchler *et al.*, 2011).

DISCUSSION

The association of *FLG* mutations with ichthyosis vulgaris and AD is well established (Brown and McLean, 2012). However, the exact mechanism leading from genetic defects to clinical manifestation and the overall impact of these mutations are still ambiguous (Brown and McLean, 2012). To investigate the impact of FLG on the skin barrier formation, we developed an *in vitro* FLG-deficient skin construct by knocking down its

expression in primary, human keratinocytes using small interfering RNA (Küchler *et al.*, 2011). In this study, we elucidated the influence of FLG on the skin lipid formation and composition and the acidification mechanism in FLG-deficient constructs in a time-dependent manner. The advantage of *in vitro FLG* knockdown constructs is that we are able to investigate the influence of FLG alone without other possibly contributing factors.

In terms of skin lipid organization, we found less ordered intercellular lipid lamellae in *FLG*− constructs compared to the normal constructs at day 14, indicating a decreased viscosity and higher degree of freedom of mobility of the lipid chains. A similar decrease in lipid chain order was found in non-lesional SC from patients with AD and psoriasis (Wohlrab *et al.*, 2001). This disorder was accompanied by a significantly higher permeability for lipophilic drugs in *FLG*− skin constructs at day 14 (Küchler *et al.*, 2011), which is in agreement with (Potts and Francoeur, 1990). These results correspond well with the observed changes in sPLA activity (upregulation at day 14), fatty acid level (increase at day 14), and skin lipid order (decreased at day 14) in *FLG*−. In contrast, no differences in permeability were found at day 7.

When considering the lipid chain packing, electron diffraction showed a higher proportion of hexagonal compared to orthorhombic lateral chain packing in AD patients (Pilgram *et al.*, 2001). However, we were unable to confirm this finding as our *in vitro* constructs generally did not form the orthorhombic lipid lattice. This is well in accordance with findings from other skin constructs (Thakoersing *et al.*, 2012).

First, we assumed that the changes in the lipid chain order must be related to a decrease in Cer levels in the *FLG*− constructs. Such a lack of Cer was described repeatedly in AD patients (Di Nardo *et al.*, 1998; Bleck *et al.*, 1999; Imokawa, 2009; Ishikawa *et al.*, 2010). The lack of FLG and, thus, the impairment of the UCA/PCA acidification pathway may affect the activity of the Cer-generating enzymes GCerase and SMase that need an acidic pH (Fluhr and Elias, 2002). On the other hand, comparable Cer levels in AD and healthy skin were also found *in vivo* (Farwanah *et al.*, 2005). Although our lipid analyses showed lower levels of Cer in the *FLG*− constructs, this was neither statistically significant nor consistently found in the individual tissues. Therefore, there must be additional mechanism independent of *FLG* mutations leading to Cer deficiency. This is in agreement with recent reports (Jakasa *et al.*, 2011; Janssens *et al.*, 2011). The ability to generate Cer from their precursors can be explained by increased sPLA$_2$ and/or NHE-1 activity, which acidify the SC in the absence of UCA/PCA and, thus, ensure the activity of GCerase and SMase (Fluhr *et al.*, 2010).

The Cer profiles were similar in both constructs; we only found a slight decrease in total sphingosine-based Cer in *FLG*− compared to with *FLG*+. This seems to be contradictory to the lower abundances in Cer NP and total Cer EO in AD patients (Janssens *et al.*, 2011). However, in that study, patients with the most prevalent *FLG* mutations were excluded, suggesting that those changes were FLG independent. Unfortunately, only some of our constructs contained detectable amounts of the EO-type Cer; thus, we could not

study whether FLG knockdown contributes to the decrease of these extremely long acylCer found previously in AD (Park *et al.*, 2012). Notably, neither GSph nor SPC were detected in the skin constructs. These lysolipids are formed from GCer and SM, respectively, by the action of GCer-SM-deacylase, which is highly expressed in the skin of AD patients. The breakdown of these Cer precursors leads to Cer deficiency and barrier disruption (Hara *et al.*, 2000; Ishibashi *et al.*, 2003). Our data suggest that there is no link between FLG and GCer-SM-deacylase in AD, both can independently contribute to skin lipid barrier abnormalities.

The most striking feature in the SC lipid profiles of our skin constructs was the almost 2-fold increase of the FFA fraction in *FLG*− compared to *FLG*+ at day 14 strongly suggesting an involvement of sPLA$_2$ as an alternative acidification pathway. Indeed, at day 14 we observed a significant increase of sPLA$_2$ IIA in *FLG*− constructs and an about 55% increased sPLA$_2$ activity explaining the high amounts of FFA. This is in line with previous *in vivo* findings: two times higher FFA levels were found in atopic epidermis (1.30 ± 0.74 mg g^{-1} wet weight) compared to healthy epidermis (0.61 ± 0.14 mg g^{-1}) (Schäfer and Kragballe, 1991). Furthermore, Tarroux *et al.* (2002) found significantly increased sPLA activity in atopic skin and a decrease in activity upon treatment. The increased production of FFA because of sPLA$_2$ IIA upregulation not only disturbs the lipid ratio and lipid order in the skin barrier but also directly contributes to inflammatory processes (Chan and Mauro, 2011).

Because these changes were detected only at day 14, we further investigated the time course of the pH values of the skin constructs. Interestingly, we found a physiological pH of about 5.5 from day 4 through day 14 of tissue cultivation in both constructs, suggesting that other mechanisms than FLG maintain the SC acidity in the absence of FLG. Initially, at day 4, the basal activity of NHE-1 is fully sufficient to maintain the acidic pH. This idea is substantiated by the high abundance of NHE-1 in the skin constructs already at day 4. This result is in good agreement with previous findings that FLG-UCA/PCA pathway is not essential for SC acidification (Fluhr *et al.*, 2010) and that NHE-1 is the primary source of acidic microdomains activating lipid processing enzymes (Behne *et al.*, 2002).

At day 7, the lack of FLG becomes apparent as UCA/PCA values are significantly lower in *FLG*− constructs (Supplementary Figure S4 online). NHE-1 is still able to maintain an acidic pH but is significantly upregulated in *FLG*−, which is likely a compensatory mechanism of the decreased UCA/PCA-based acidity. At this time point, *FLG*+ and *FLG*− constructs are still very similar as also indicated by the skin lipid arrangement and permeability being in a good agreement with (Mildner *et al.*, 2010), who cultivated their models for 7 days. The most pronounced consequences of FLG deficiency appear at later time points because of the progressive differentiation and maturation of the skin constructs. At day 14, NHE-1 is still upregulated in *FLG*− constructs but yet another acidification mechanism is activated: the PL-FFA conversion by sPLA$_2$. The importance of NHE-1 and sPLA$_2$ for skin acidification has been demonstrated before (Fluhr *et al.*, 2001, 2004). While this happens in both *FLG*− and
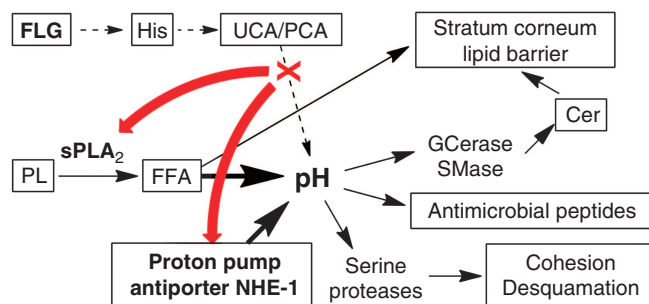
Figure 5. Stratum corneum pH unifying concept. In filaggrin (FLG) deficiency, sodium/hydrogen antiporter (NHE-1) and secretory phospholipase A₂ (sPLA₂) are upregulated to maintain the acidic pH needed for a variety of skin functions. Adapted and modified from Fluhr *et al.* (2002). Cer, ceramide; FFA, free fatty acid; GCerase, β-glucocerebrosidase; His, histidine; NHE-1, sodium/hydrogen antiporter; PCA, pyrrolidone-5-carboxylic acid; SMase, sphingomyelinase; UCA, urocanic acid.

FLG+ constructs, the expression and activity of sPLA₂ are significantly higher in the *FLG*−. Thus, although the time course of NHE-1- and FFA-based acidification pattern of the skin constructs is not affected by deficient FLG, these two pathways are upregulated to compensate for the lack of FLG-His-UCA/PCA.

The question is what exactly is the trigger activating the other acidification pathways. As we did not detect any differences in pH between *FLG*+ and *FLG*−, it seems that these compensatory mechanisms are activated by very small or localized pH changes that we are not able to measure. Another possibility is that acidification is controlled not by pH itself but by the levels of products or intermediates of other acidification pathways. The latter possibility would be more advantageous as it would prevent pH changes rather than correct them.

Nevertheless, we cannot exclude that there are other key players involved in the acidification process that have not yet been identified as also suggested by Behne *et al.* (2002). Our findings are well in line with Fluhr *et al.* (2010) and substantiate the idea of compensatory mechanism between different pathways to ensure skin acidification.

In conclusion, the decreased levels of UCA/PCA accompanied by an increase of NHE-1 and later sPLA₂ IIA in *FLG*− constructs demonstrate an interplay between different skin acidification pathways. Figure 5 displays the suggested processes of skin acidification. In addition, using *in vitro* skin constructs, we showed that FLG deficiency directly influences the skin lipid orientation by increasing the amount of FFA and, thus, affecting skin permeability. Our results considerably contribute to the understanding of skin acidification and the impact of FLG deficiency on skin barrier dysfunction. To our best knowledge, these direct interdependencies have not been described before.

MATERIALS AND METHODS

Cer NS and AS, GCer, SM, GSph, and SPC were purchased from Avanti Polar Lipids (Alabaster, AL). Cer NP was prepared by acylation of phytosphingosine with lignoceric acid as described previously

(Novotny *et al.*, 2009a, 2009b). The structure and purity of the prepared Cer NP were confirmed by ^{1}H and ^{13}C nuclear magnetic resonance spectra (Varian, Palo Alto, CA, Mercury-Vx BB 300 instrument, operating at 300 MHz for ^{1}H, 75 MHz for ^{13}C), MS (Agilent 500 Ion Trap LC/MS, Santa Clara, CA), and infrared spectra (Nicolet 6700 FTIR spectrophotometer, Thermo Scientific, Waltham, MA). Chol and all other chemicals were from Sigma-Aldrich (Schnelldorf, Germany). Radiolabeled 1,2,6,7-^{3}H-testosterone was from Amersham (Freiburg, Germany). Radiolabeled 1-methyl-^{14}C-caffeine was from Arc (St Louis, MO).

Preparation of skin constructs

The skin constructs (*FLG*+ and *FLG*−) have been generated according to Eckl *et al.* (2011) and Küchler *et al.* (2011). SC was isolated after 4, 7, and 14 days. The constructs were placed on a filter paper soaked in 0.5% trypsin in phosphate-buffered saline (PBS, pH 7.4) (Kligman and Christophers, 1963). The isolated SC sheets were washed with PBS and any remaining keratinocytes were removed with a cotton swab. Subsequently, SC sheets were washed with acetone to remove surface contaminants, vacuum-dried, and stored at −20 °C. Isolated human SC served as control.

FTIR spectroscopy

IR spectra of the samples were collected on a Nicolet 6700 FTIR spectrometer (Thermo Scientific) equipped with a single-reflection MIRacle attenuated total reflectance germanium crystal at 23 °C. The spectra were generated by coaddition of 256 scans collected at 4 cm^{-1} resolution and analyzed with the Bruker OPUS software (Bruker Corp, Billerica, MA). The exact peak positions were determined from second derivative spectra and by peak fitting if needed.

Isolation of SC lipids

For the extraction of the SC intercellular lipids, a modified (Bligh and Dyer, 1959) method was used. The SC samples were extracted with 1 ml CHCl₃/MeOH 2:1 (v/v) per mg of SC for 1.5 hours, filtered, separated, and concentrated under a stream of nitrogen. The lipids were dried and stored at −20 °C under argon.

High-performance thin-layer chromatography lipid analysis

The lipid analysis was performed on silica gel 60 high-performance thin-layer chromatography plates (20 × 10 cm²; Merck, Darmstadt, Germany). The extracted SC lipids were dissolved in 100 µl CHCl₃/MeOH 2:1. Ten microliters of each lipid sample was sprayed on the plate using a Linomat IV (Camag, Muttenz, Switzerland). Standard lipids were dissolved in CHCl₃/MeOH 2:1 (v/v) (Cer NS, AS, NP, Chol, and palmitic acid), CHCl₃/MeOH 1:1 (v/v) (CholS, GCer, and SM), and MeOH GSph and SPC), respectively, at 1 mg ml^{-1}. They were first analyzed separately during method development and then mixed at 50 µg ml^{-1} and applied on an high-performance thin-layer chromatography plate together with the analyzed samples to generate calibration curves from 50 ng to 7.5 µg. The major skin barrier lipids (Cer, FFA, and Chol) were separated using CHCl₃/MeOH/acetic acid 190:9:1.5 (v/v/v) mobile phase two times to the top of the plate (Bleck *et al.*, 1999). The Cer precursors (GCer and SM), their degradation products (GSph and SPC), and CholS were separated using a more polar mobile phase (CHCl₃/MeOH/acetic acid/H₂O 65:25:6:3 (v/v/v/v)).

The lipids were visualized by dipping in a derivatization reagent (7.5% $CuSO_4$, 8% H_3PO_4, and 10% MeOH in water) for 10 seconds and heating at 160 °C for 30 minutes and quantitated by densitometry using TLC scanner 3 and WinCats software (Camag, Muttenz, Switzerland).

Determination of FLG, sPLA$_2$, and NHE-1 expression

For isolation of RNA, the constructs were harvested at day 14 and punched to discs (10 mm). Epidermis was frozen using liquid nitrogen and then milled for 30 seconds at 25 Hz using a TissueLyzer (Qiagen, Hilden, Germany). Subsequently, RNA was isolated using Nucleo Spin RNA II according to the manufacturer's instruction. For cDNA synthesis, RevertAid First Strand cDNA Synthesis Kit (Thermo Scientific) was used according to the manufacturer's instruction.

For relative quantification of FLG, NHE-1, and sPLA$_2$ isoforms' expression, reverse transcription PCR was performed using the SYBR Green I Masterplus kit (Roche, Penzberg, Germany). For primer sequences see Supplementary Table S2 online. The housekeeping gene *YWHAZ* served as control.

Skin surface pH measurements

Luminescent 2D imaging of pH (Meier *et al.*, 2011; Schreml *et al.*, 2011) was performed via RGB imaging (Meier *et al.*, 2011) of pH sensor foils consisting of a hydrogel layer containing pH indicator microparticles (FITC bound to aminoethylcellulose) and reference particles (ruthenium(II)-tris(4,7-diphenyl-1,10-phenanthroline) incorporated in polyacrylonitrile). Sensor foils were gently applied to the 3D skin construct surfaces and were allowed to slowly adapt by adhesion forces. Calculations and pseudocolor image processing were carried out with ImageX software (Microsoft Corporation, Redmond, WA) and ImageJ (http://rsbweb.nih.gov/ij/). For details see Supplementary methods online.

Immunohistochemistry

After 14 days, the constructs were embedded in tissue freezing medium (Leica Microsystems, Nussloch, Germany) and frozen using liquid nitrogen. After overnight storage at − 80 °C, the constructs were cut to vertical slices (5 µm) with a freeze microtome (Leica Microsystems, Nussloch, Germany). After fixation, they were washed with PBS containing 1% BSA and blocked with normal goat serum (1:20 in PBS). The sections were incubated for 1 hour with primary rabbit antibodies specific against NHE-1 and sPLA$_2$ IIA (Abcam, Cambridge, UK) diluted in PBS containing 1% BSA (1:400 and 1:200, respectively) and subsequently with goat-anti-rabbit IgG DyLight 488 antibody (Dianova, Hamburg, Germany). After washing, the sections were embedded in antifading mounting medium (Dianova) and analyzed with a fluorescence microscope (BZ-8000; Keyence, Neu-Isenburg, Germany).

Skin permeability testing

The skin permeability was evaluated according to validated test procedures (Schäfer-Korting *et al.*, 2008). Briefly, stock solutions of testosterone (40 µg ml^{-1}, 2% (v/v) Igepal CA-630) and caffeine (1 mg ml^{-1}) were spiked with an appropriate amount of the radiolabelled compound to achieve a total radioactivity of 2 µCi ml^{-1}. Permeation studies were performed at day 7 using a static setup (Franz-type diffusion cells, diameter 15 mm, volume 12 ml; Permegear, Bethlehem, PA).

Statistical analysis

Wilcoxon's signed-rank test or *t*-test were used when comparing two different conditions according to the results of D'Agostino–Pearson normality test. When comparing three or more conditions, a one-way analysis of variance with a Bonferroni *post hoc* test or Friedman plus Dunn's tests was performed using SigmaStat for Windows 3.5 (SPSS, Chicago, IL). $P \leqslant 0.05$ was considered significant. The data are presented as means ± SEM.

SUPPLEMENTARY MATERIAL
Supplementary material is linked to the online version of the paper at http://www.nature.com/jid

REFERENCES

Behne MJ, Meyer JW, Hanson KM *et al.* (2002) NHE1 regulates the stratum corneum permeability barrier homeostasis. Microenvironment acidification assessed with fluorescence lifetime imaging. *J Biol Chem* 277:47399–406

Bleck O, Abeck D, Ring J *et al.* (1999) Two ceramide subfractions detectable in Cer(AS) position by HPTLC in skin surface lipids of non-lesional skin of atopic eczema. *J Invest Dermatol* 113:894–900

Bligh EG, Dyer WJ (1959) A rapid method of total lipid extraction and purification. *Can J Biochem Physiol* 37:911–7

Brown SJ, McLean WH (2012) One remarkable molecule: filaggrin. *J Invest Dermatol* 132:751–62

Chan A, Mauro T (2011) Acidification in the epidermis and the role of secretory phospholipases. *Dermatoendocrinol* 3:84–90

Di Nardo A, Wertz P, Giannetti A *et al.* (1998) Ceramide and cholesterol composition of the skin of patients with atopic dermatitis. *Acta Dermatol Venereol* 78:27–30

Eckl KM, Alef T, Torres S *et al.* (2011) Full-thickness human skin models for congenital ichthyosis and related keratinization disorders. *J Invest Dermatol* 131:1938–42

Farwanah H, Raith K, Neubert RH *et al.* (2005) Ceramide profiles of the uninvolved skin in atopic dermatitis and psoriasis are comparable to those of healthy skin. *Arch Dermatol Res* 296:514–21

Feingold KR (2007) Thematic review series: skin lipids. The role of epidermal lipids in cutaneous permeability barrier homeostasis. *J Lipid Res* 48:2531–46

Fluhr JW, Behne MJ, Brown BE *et al.* (2004) Stratum corneum acidification in neonatal skin: secretory phospholipase A2 and the sodium/hydrogen antiporter-1 acidify neonatal rat stratum corneum. *J Invest Dermatol* 122:320–9

Fluhr JW, Elias PM (2002) Stratum corneum pH: formation and function of the 'Acid Mantle'. *Exogen Dermatol* 1:163–75

Fluhr JW, Elias PM, Man MQ *et al.* (2010) Is the filaggrin–histidine–urocanic acid pathway essential for stratum corneum acidification? *J Invest Dermatol* 130:2141–4

Fluhr JW, Kao J, Jain M *et al.* (2001) Generation of free fatty acids from phospholipids regulates stratum corneum acidification and integrity. *J Invest Dermatol* 117:44–51

Hara J, Higuchi K, Okamoto R *et al.* (2000) High-expression of sphingomyelin deacylase is an important determinant of ceramide deficiency leading to barrier disruption in atopic dermatitis. *J Invest Dermatol* 115:406–13

Imokawa G (2009) A possible mechanism underlying the ceramide deficiency in atopic dermatitis: expression of a deacylase enzyme that cleaves the N-acyl linkage of sphingomyelin and glucosylceramide. *J Dermatol Sci* 55:1–9

Imokawa G, Abe A, Jin K *et al.* (1991) Decreased level of ceramides in stratum corneum of atopic dermatitis: an etiologic factor in atopic dry skin? *J Invest Dermatol* 96:523–6

Ishibashi M, Arikawa J, Okamoto R *et al.* (2003) Abnormal expression of the novel epidermal enzyme, glucosylceramide deacylase, and the accumulation of its enzymatic reaction product, glucosylsphingosine, in the skin of patients with atopic dermatitis. *Lab Invest* 83:397–408

Ishikawa J, Narita H, Kondo N *et al.* (2010) Changes in the ceramide profile of atopic dermatitis patients. *J Invest Dermatol* 130:2511–4

Jakasa I, Koster ES, Calkoen F *et al.* (2011) Skin barrier function in healthy subjects and patients with atopic dermatitis in relation to filaggrin loss-of-function mutations. *J Invest Dermatol* 131:540–2

Janssens M, van Smeden J, Gooris GS *et al.* (2011) Lamellar lipid organization and ceramide composition in the stratum corneum of patients with atopic eczema. *J Invest Dermatol* 131:2136–8

Jung T, Stingl G (2008) Atopic dermatitis: therapeutic concepts evolving from new pathophysiologic insights. *J Allergy Clin Immunol* 122:1074–81

Kligman AM, Christophers E (1963) Preparation of isolated sheets of human stratum corneum. *Arch Dermatol* 88:702–5

Krien PM, Kermici M (2000) Evidence for the existence of a self-regulated enzymatic process within the human stratum corneum—an unexpected role for urocanic acid. *J Invest Dermatol* 115:414–20

Küchler S, Henkes D, Eckl KM *et al.* (2011) Hallmarks of atopic skin *in vitro* mimicked by the means of a skin disease model based on FLG knock down. *Altern Lab Anim* 39:471–80

Meier RJ, Schreml S, Wang XD *et al.* (2011) Simultaneous photographing of oxygen and pH *in vivo* using sensor films. *Angew Chem* 50:10893–6

Mendelsohn R, Moore DJ (2000) Infrared determination of conformational order and phase behavior in ceramides and stratum corneum models. *Methods Enzymol* 312:228–47

Mildner M, Jin JA, Eckhart L *et al.* (2010) Knockdown of filaggrin impairs diffusion barrier function and increases UV sensitivity in a human skin model. *J Invest Dermatol* 130:2286–94

Novotny J, Janusova B, Novotny M *et al.* (2009a) Short-chain ceramides decrease skin barrier properties. *Skin Pharmacol Physiol* 22:22–30

Novotny J, Pospechova K, Hrabalek A *et al.* (2009b) Synthesis of fluorescent C24-ceramide: evidence for acyl chain length dependent differences in penetration of exogenous NBD-ceramides into human skin. *Bioorg Med Chem Lett* 19:6975–7

O'Regan GM, Sandilands A, McLean WH *et al.* (2009) Filaggrin in atopic dermatitis. *J Allergy Clin Immunol* 124:R2–6

Palmer CNA, Irvine AD, Terron-Kwiatkowski A *et al.* (2006) Common loss-of-function variants of the epidermal barrier protein filaggrin are a major predisposing factor for atopic dermatitis. *Nat Genet* 38441–6

Pappinen S, Hermansson M, Kuntsche J *et al.* (2008) Comparison of rat epidermal keratinocyte organotypic culture (ROC) with intact human skin: lipid composition and thermal phase behavior of the stratum corneum. *Biochim Biophys Acta* 1778:824–34

Park YH, Jang WH, Seo JA *et al.* (2012) Decrease of ceramides with very long-chain fatty acids and downregulation of elongases in a murine atopic dermatitis model. *J Invest Dermatol* 132:476–9

Pilgram GS, Vissers DC, van der Meulen H *et al.* (2001) Aberrant lipid organization in stratum corneum of patients with atopic dermatitis and lamellar ichthyosis. *J Invest Dermatol* 117:710–7

Ponec M (2002) Skin constructs for replacement of skin tissues for *in vitro* testing. *Adv Drug Delivery Rev* 54:S19–30

Potts RO, Francoeur ML (1990) Lipid biophysics of water loss through the skin. *Proc Natl Acad Sci USA* 87:3871–3

Rawlings AV, Harding CR (2004) Moisturization and skin barrier function. *Dermatol Ther* 17(Suppl 1):43–8

Schäfer L, Kragballe K (1991) Abnormalities in epidermal lipid metabolism in patients with atopic dermatitis. *J Invest Dermatol* 1:10–5

Schäfer-Korting M, Bock U, Diembeck W *et al.* (2008) The use of reconstructed human epidermis for skin absorption testing: results of the validation study. *Altern Lab Anim* 36:161–87

Schreml S, Meier RJ, Wolfbeis OS *et al.* (2011) 2D luminescence imaging of pH *in vivo*. *Proc Natl Acad Sci USA* 108:2432–7

Tarroux R, Assalit MF, Licu D *et al.* (2002) Variability of enzyme markers during clinical regression of atopic dermatitis. *Skin Pharmacol Appl Skin Physiol* 1:55–62

Thakoersing VS, Gooris GS, Mulder A *et al.* (2012) Unraveling barrier properties of three different in-house human skin equivalents. *Tissue Eng Part C* 18:1–11

Velkova V, Lafleur M (2002) Influence of the lipid composition on the organization of skin lipid model mixtures: an infrared spectroscopy investigation. *Chem Phys Lipids* 117:63–74

Wertz PW (2000) Lipids and barrier function of the skin. *Acta Derm Venereol Suppl (Stockh)* 208:7–11

Wohlrab J, Vollmann A, Wartewig S *et al.* (2001) Noninvasive characterization of human stratum corneum of undiseased skin of patients with atopic dermatitis and psoriasis as studied by Fourier transform Raman spectroscopy. *Biopolymers* 62:141–6